

# Putting small strain non-linearity into Modified Cam Clay model

M.D. Bolton, G.R. Dasari & A.M. Britto  
Cambridge University, Engineering Department, UK

**ABSTRACT:** Overconsolidated clays exhibit non-linear stress-strain behaviour at small strains prior to gross plastic yielding. The effect of mean normal effective stress, deviatoric strain and overconsolidation ratio on the shear modulus is assessed from the results of laboratory triaxial tests at small strains. A general form of power function for shear modulus is derived and its implementation inside the yield surface of the Modified Cam Clay model within the CRISP finite element program is described. Simulation of triaxial tests, and ground movements due to tunnelling are compared with appropriate data and contrasted with constant stiffness analyses.

## 1 INTRODUCTION

A major concern in design of structures such as diaphragm walls and tunnels in overconsolidated clays is the magnitude of ground movement. It has been reported that such structures typically mobilise a maximum shear strain of 0.2% (Simpson et al., 1979). Overconsolidated clays exhibit non-linear stress-strain behaviour at these small strains prior to gross plastic yielding (Jardine et al., 1984; Atkinson et al., 1990; Viggiani, 1992). Therefore, the accurate modelling of stress-strain behaviour at small strains is very important to an analysis of structures in overconsolidated clays. In the existing version of the Modified Cam Clay (MCC) model (Roscoe and Burland, 1968) elastic shear strains are assumed to be zero i.e. shear modulus is infinite. But this leads to problems in its implementation in a finite element program like CRISP (CRITICAL State Program). So, there are two options in CRISP- constant Poisson's ratio or constant shear modulus (Britto and Gunn, 1987). For a constant Poisson's ratio the MCC model invokes a shear modulus which is calculated to be proportional to bulk modulus using linear elasticity inside the yield surface. The elastic shear modulus is then given by

$$G = \frac{3(1-2\nu) V p'}{2(1+\nu) \kappa} \quad (1)$$

where  $\nu$  is Poisson's ratio,  $V$  is specific volume,  $p'$  is mean normal effective pressure and  $\kappa$  is the slope of unloading/reloading line in  $V-\ln p'$  space. Variation of shear modulus with shear strain and overconsolidation ratio has, therefore, been ignored in the MCC model.

## 2 MODELLING OF SHEAR MODULUS

Many constitutive relations model soil as either elastic or elasto-plastic, both use a shear modulus. The problem then is the selection of a value for the shear modulus. Data shows that the shear modulus is not constant but varies, depending on the stress state of the soil (Ladd, 1964; Hardin and Black, 1968; Hardin and Drnevich, 1972; Houlsby and Wroth, 1991). Ignoring the effect of vibration frequency, temperature, incomplete saturation etc., the shear modulus for overconsolidated clays at small strains may be expressed in the form of

$$G = f(p', \text{OCR}, \epsilon_q) \quad (2)$$

where OCR is the overconsolidation ratio defined as  $(p_c / p')$ ,  $p_c$  is the pre-consolidation pressure and  $\epsilon_q$  is the deviatoric strain.

The accurate measurement of the soil stiffness at small strains has been reported by many researchers (Jardine et al., 1984; Clayton et al., 1988, Goto et al., 1991 and Viggiani, 1992). The results obtained from small strain triaxial tests by Viggiani (1992) on Speswhite kaolin will be used here because centrifuge data are available for many boundary value problems in kaolin. Details of the tests and small strain measurements using bender elements are given in Viggiani (1992). The variation of shear modulus with deviatoric strain for kaolin is shown in Fig. 1.

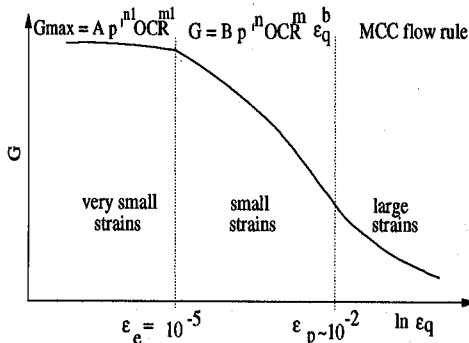


Fig. 1 Typical stiffness-strain curve for kaolin

At very small strains, the tangent shear modulus of soil appears to be constant at  $G_{max}$  for a given OCR and  $p'$  up to a deviatoric strain,  $\epsilon_e$ , which is at the threshold of elastic behaviour. Below this threshold, it will be assumed that:

$$G_{max} = A p'^{n1} OCR^{m1} \quad (3)$$

and for  $\epsilon_e < \epsilon_q < \epsilon_p$  the tangent shear modulus  $G$  is assumed to be in the form of

$$G = B p'^n OCR^m \epsilon_q^b \quad (4)$$

where  $A$ ,  $B$ ,  $n1$ ,  $m1$ ,  $n$ ,  $m$ , and  $b$  are soil parameters derived from triaxial tests, and  $\epsilon_p$  represents the onset of plastic yielding on the Cam Clay yield surface.

Viggiani's kaolin clay samples were subjected to a number of isotropic compression and swelling stress paths. The maximum tangent shear modulus ( $G_{max}$ ) for a known  $p'$  and OCR was measured at very small strains ( $<10^{-5}$ ). The data shows that  $G_{max}$  increases with both  $p'$  and OCR, though not in a linear fashion. The soil parameters  $A$ ,  $n1$  and  $m1$  were derived by Viggiani (1992) from the measured  $G_{max}$  using equation (3) and these are shown in Table 1 (stress units are kPa)

Table: 1 Parameters for Speswhite kaolin

A	n1	m1
1964	0.65	0.2

For OCR = 1, equation (4) reduces to

$$G = B p'^n \epsilon_q^b \quad (5)$$

Equation (5) can be used to plot the results from OCR = 1 tests. As shown in Fig. 2,  $G$  and  $p'$  are plotted on logarithmic axes at various deviatoric strains. The slope of the graph gives a value of pressure exponent ' $n$ '. As seen from Fig. 2 ' $n$ ' increases with deviatoric strain. An average value of  $n = 0.8$  was selected.

The same data are re-plotted in Fig. 3 for shear modulus versus deviatoric strain at various mean normal effective pressures. The shear modulus decreases with deviatoric strain for a given  $p'$ . The slope of any line gives a value of strain exponent ' $b$ '. As shown ' $b$ ' increases with  $p'$ , but it was decided to use an average value of  $b = -0.65$ .

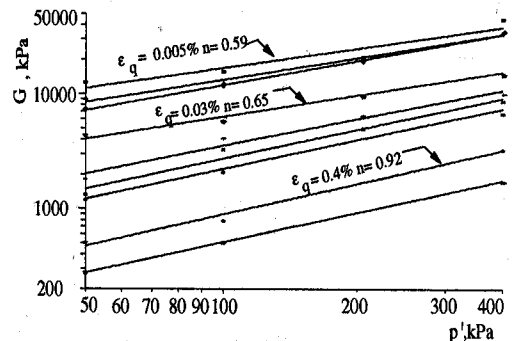


Fig 2 Relation between shear modulus and mean normal effective stress for various deviatoric strains

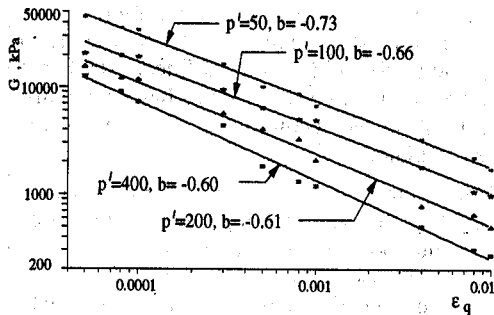


Fig 3 Relation between shear modulus and deviatoric strain for various mean normal effective stresses

Equation (4) can be expressed as

$$G = C p'^n \epsilon_q^b \quad (6)$$

where  $C = B \text{OCR}^m$ . Then

$$C = G / (p'^n \epsilon_q^b) \quad (7)$$

and a graph between  $C$  and  $\text{OCR}$  give values of  $B$  and  $m$  as shown Fig. 4.

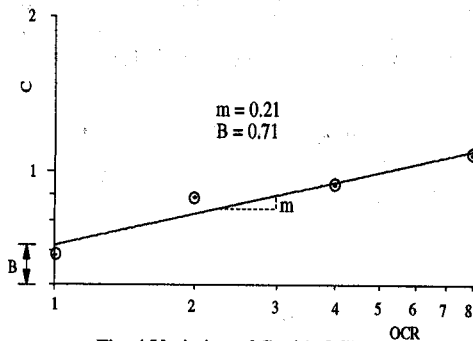


Fig. 4 Variation of C with OCR

Therefore, at very small strains ( $< 10^{-5}$ ), shear modulus of kaolin is given by

$$G_{\max} = 1964 p'^{0.65} \text{OCR}^{0.20} \quad (8)$$

and for strains more than  $10^{-5}$  shear modulus is given by

$$G = 0.71 p'^{0.8} \text{OCR}^{0.23} \epsilon_q^{-0.65} \quad (9)$$

### 3 SMALL STRAIN MODEL IN CRISP

The Strain Dependent Modified Cam Clay (SDMCC) model has been incorporated in to the finite element program CRISP. It needs the following additional input

- $\epsilon_e$ ,  $A$ ,  $n1$  and  $m1$  to calculate  $G_{\max}$
- $B$ ,  $n$ ,  $m$  and  $b$  to calculate  $G$

where  $\epsilon_e$  is the value of deviatoric strain below which the shear stiffness is assumed to be strain independent. The shear modulus inside the yield surface of the SDMCC model is calculated using equation (8) or (9) depending on the magnitude of deviatoric strain. Bulk modulus is calculated as in the MCC model.

On the yield surface, plasticity and the associated flow rule govern the stress-strain behaviour of soil. The elastic shear strains during yielding are generally very small compared to the plastic strains. Hence the shear modulus is calculated with equation (8). Then the global stiffness matrix is calculated and equations are solved for displacements, stresses, strains, pore pressures etc., similar to any other finite element program.

### 4 RESULTS FROM TRIAXIAL TESTS

The results obtained from CRISP using the MCC model and the SDMCC model for overconsolidated clay are compared with experimental results in Fig. 5. As can be seen, for overconsolidated clays inside the yield surface for a constant  $p'$ , the shear modulus predicted by the MCC model is constant (strain independent). The shear modulus predicted by the SDMCC model varies from about 52000 kPa to a very small value depending on the deviatoric strain for this test. If a problem involves small strains ( $< 0.0005$ ), the shear modulus is under estimated by the MCC model. The shear modulus for intermediate and large strains is over estimated by the MCC model.

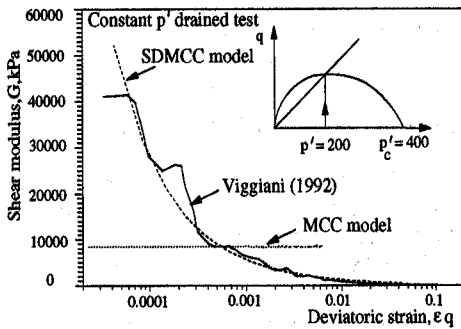


Fig. 5 Shear modulus prediction for OCC

### 5 GROUND MOVEMENTS DUE TO TUNNELLING

The surface settlement profiles predicted by the MCC model in overconsolidated clays are much shallower and wider than those observed in centrifuge model tests (Mair, 1979). The reason for this is the small strain part of the constitutive model, where the shear modulus was taken to be strain independent.

Here, a centrifuge test done by Mair (1979) is analysed by the MCC model and the SDMCC model. A short description of the test procedure is given here and details are given in Mair (1979). The kaolin sample was pre-consolidated to 171 kN/m<sup>2</sup> and a model of 180 mm x 150 mm x 315 mm size was prepared. The model was instrumented, mounted on the Cambridge beam centrifuge and acceleration was increased up to 75g. Once equilibrium (dissipation of negative excess pore pressures) was reached, the centrifuge was stopped and the tunnel was cut. The tunnel diameter was 60 mm. The tunnel axis was 130 mm below the top surface with a cover to diameter ratio of 1.67. Fig. 6 gives the dimensions of the tunnel at prototype scale. The centrifuge was restarted and the tunnel support pressure (150 kPa) applied gradually as the centrifuge acceleration increased to 75g. Then the tunnel pressure was very quickly reduced. Pore pressures and displacements were measured during this whole operation.

CRISP analysis started from the equilibrium stage in the centrifuge at prototype scale. The in-situ vertical and horizontal effective stresses and pore pressures were entered in to the program. During the equilibration, excess pore

pressures dissipate as the soil swells. Two types of analysis were performed. In the first case, in-situ strains corresponding to the equilibrium stage are calculated integrating equations (8) and (9) along a linear stress path connecting the two stress states before and after swelling. In the second case, no in-situ strains are calculated.

The tunnel construction is modelled by removing the elements representing the tunnel in a number of increments and the tunnel support pressure was applied simultaneously. Then the tunnel support pressure was quickly reduced in an undrained condition. The preliminary results showed that displacement profiles in the far field were significantly affected by the yielding behaviour of elements around the tunnel. Fig. 6 shows the principal stress directions due to reduction of tunnel pressure. The soil elements near crown and invert of the tunnel are under vertical extension and soil elements near the springings are under vertical compression. Hence it was considered appropriate to assign different values of 'M' (compression M=0.9, extension M=0.8) to these elements, as reported in appropriate plane strain tests on kaolin (Sketchley, 1973). Table 2 gives the Cam Clay parameters used in the analysis.

The surface settlements predicted by the MCC and the SDMCC models, with and without in-situ strains at two different tunnel

Table 2 Cam Clay parameters

$\lambda$	$\kappa$	M	$\Gamma$	$\nu$
0.3	0.05	0.9/0.8	3.92	0.33

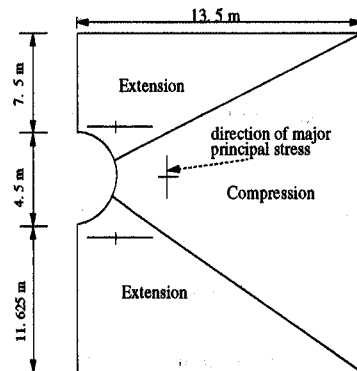


Fig.6 Tunnel with stress path directions

pressures, are shown in Fig. 7 and Fig. 8. The MCC model predicts small movements because the shear modulus predicted is high at moderate strains ( $> 0.01$ ), see Fig. 5. The displacement profiles predicted by the MCC model are flatter since shear modulus is strain independent. The surface settlements are reasonably well predicted by the SDMCC model when in-situ strains corresponding to the equilibrium stage are calculated. The settlement profiles predicted by the SDMCC model are deeper and shallower than the MCC model predictions.

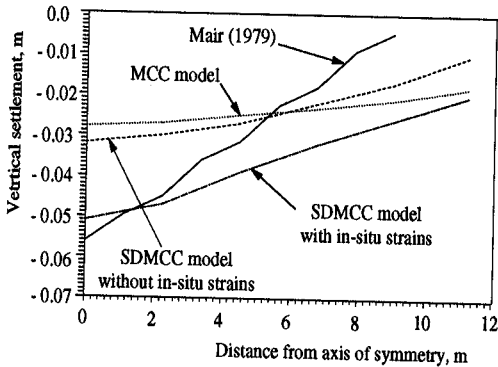


Fig. 7 Surface displacement profile (tunnel pressure 107 kPa)

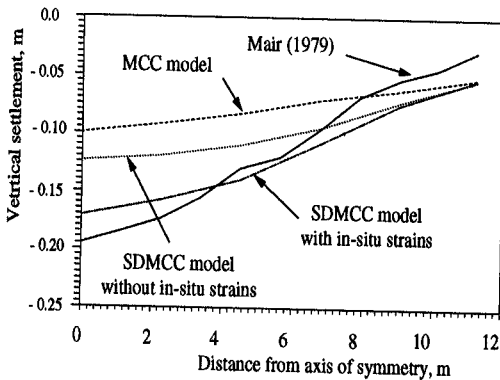


Fig. 8 Surface displacement profile (tunnel pressure 76 kPa)

The increase in vertical settlement of a point directly above the tunnel crown (mid surface) as the tunnel pressure reduces, is shown in Fig. 9. The movement of the point is satisfactorily predicted by the SDMCC model. Pore pressure predictions are similar in all cases. The displacement profiles and

movement of mid surface are well predicted when in-situ strains are calculated. This raises a question: whether to attempt to calculate in-situ strains in the field or not.

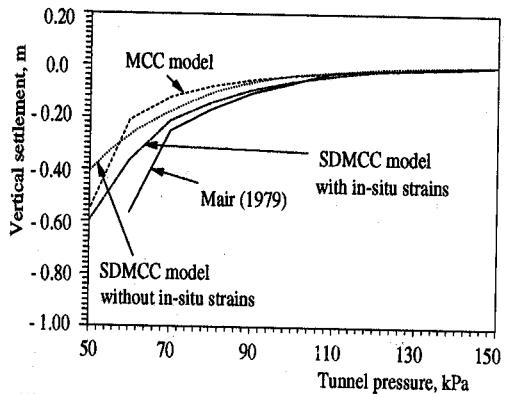


Fig. 9 Tunnel pressure versus mid-surface settlement

## 6 CONCLUSIONS

A strain-dependent shear stiffness has been incorporated for Modified Cam Clay model within the yield surface. Based on power functions of  $p'$ , OCR and  $\epsilon_q$ , constant values for the exponents were selected to fit triaxial tests. The goodness of fit seemed promising, both at very small strains and large strains. The 8 new parameters for the new SDMCC model can be obtained from a minimum of three triaxial tests.

MCC and SDMCC models have been used to compare with the behaviour observed in centrifuge tests on tunnels in clay. The magnitude and shape of surface subsidence above the tunnel could not simultaneously be predicted by the MCC model. However, the SDMCC model fitted observed behaviour much better, especially when the critical stress ratio ( $M$ ) was permitted to reflect the local strain path (extension or compression) appropriate to tunnel pressure reduction.

If strain-dependent stiffness are to be used in analysis, the predictor is faced with task of estimating in-situ strains, as well as in-situ stresses. An attempt to allow for prior strain history in the centrifuge tests seemed promising. Further research is required to elucidate whether, or how, to account for strain history in the field.

## REFERENCES

- Atkinson, J.H., Richardson, D. & Stallebrass, S.E. 1990. Effect of recent stress history on the stiffness of overconsolidated soil. *Geotechnique* 40:531-540.
- Britto, A.M. & Gunn, M.J. 1987. *Critical State soil mechanics via finite elements*. Chichester: Ellis Horwood Limited.
- Clayton, C.R.I., Kathrush, S.A., Bica, A.V.D., & Siddique, A. 1988. The use of Hall effect semiconductors in geotechnical instrumentation. *Geotechnical Testing Journal*, GTJODJ:12, 69-76.
- Goto, S., Tatsuoka, F., Shibuya, S., Kim, Y.S., & Sato, T. 1991. A simple gauge for local small strain measurements in the laboratory. *Soils and Foundations*: 31, 169-180.
- Hardin, B.O. & Black, W.L. 1968. Vibration modulus of normally consolidated clay. *ASCE, JSMFD*: 95, SM6,1531-1537.
- Hardin, B.O. & Drnevich, V.P. 1972. Shear modulus and damping in soils: design equations and curves. *ASCE, JSMFD*: 98, SM7,667-692.
- Houlsby, G.T. & Wroth, C.P. 1991. The variation of shear modulus of a clay with pressure and overconsolidation ratio. *Soils and Foundations*: 31,138-143.
- Jardine, R.J., Symes, M.J. & Burland, J.B. 1984. The measurement of soil stiffness in the triaxial apparatus. *Geotechnique*: 34, 323-340.
- Ladd, C.C. 1964. Stress-strain modulus of clay in undrained shear, *ASCE, JSMFD*: 90, SM5.
- Mair, R.J. 1979. *Centrifugal modelling of tunnel construction in soft clay*. PhD thesis. Cambridge University. UK.
- Roscoe, K.H. & Burland, J.B. 1968. On the generalised stress-strain behaviour of an idealised wet clay. *Engineering Plasticity*. Cambridge University Press.
- Simpson, B., O'Riordan, N.J. & Croft, D.D. 1979. A computer model for the analysis of ground movements in London clay. *Geotechnique* 29:149-175.
- Sketchley, C.J. 1973. *The behaviour of kaolin in plane strain*. PhD thesis. University of Cambridge, UK.
- Viggiani, G. 1992. *Small strain stiffness of fine grained soils*. PhD thesis. City University. London. UK.